Original article

Nuclear Medicine Communications

^{18}F-FAZA PET/CT in pretreatment assessment of hypoxic status in high-grade glioma: correlation with hypoxia immunohistochemical biomarkers

Paola Mapelli[a,b], Marcella Callea[c], Federico Fallanca[b], Antonella Castellano[a,d], Michele Bailo[a,e], Paola Scifo[b], Valentino Bettinardi[b], Gian Marco Conte[d], Cristina Monterisi[b], Paola Maria Vittoria Rancoita[f], Elena Incerti[b], Marta Vuozzo[b], Luigi Gianolli[b], Mariarosa Terreni[c], Nicoletta Anzalone[a,d] and Maria Picchio[a,b]

Background **To investigate the correlation between ^{18}F-labeled fluoroazomycinarabinoside (18F-FAZA) PET data and hypoxia immunohistochemical markers in patients with high-grade glioma (HGG).**

Patients and methods **Prospective study including 20 patients with brain MRI suggestive for HGG and undergoing 18F-FAZA PET/CT before treatment for hypoxia assessment. For each 18F-FAZA PET scan SUV_{max}, SUV_{mean} and 18F-FAZA tumour volume (FTV) at 40, 50 and 60% threshold of SUV_{max} were calculated; hypoxic volume was estimated by applying different thresholds (1.2, 1.3 and 1.4) to tumour/blood ratio. Seventeen patients were analysed. The immunohistochemical analysis assessed the following parameters: hypoxia-inducible factor 1α, carbonic anhydrase IX (CA-IX), glucose transporter-1, tumour vascularity and Ki-67.**

Results **18F-FAZA PET showed a single lesion in 15/17 patients and multiple lesions in 2/17 patients. Twelve/17 patients had grade IV glioma and 5/17 with grade III glioma. Bioptic and surgical samples have been analysed separately. In the surgical subgroup (n=7) a positive correlation was observed between CA-IX and SUV_{max} (P=0.0002), SUV_{mean40} (P=0.0058), SUV_{mean50} (P=0.009), SUV_{mean60} (P=0.0153), FTV–40–50–60 (P=0.0424) and hypoxic volume1.2–1.3–1.4 (P=0.0058). In the bioptic group (n=10) tumour vascularisation was inversely correlated with SUV_{max} (P=0.0094), SUV_{mean40} (P=0.0107), SUV_{mean50} (P=0.0094) and SUV_{mean60} (P=0.0154).**

Conclusions **The correlation of 18F-FAZA PET parameters with CD31 and CA-IX represents a reliable method for assessing tumour hypoxia in HGG. The inverse correlation between tumour vascularisation, SUV_{max} and SUV_{mean} suggest that highly vascularized tumours might present more oxygen supply than hypoxia. *Nucl Med Commun* 42: 763–771**

Nuclear Medicine Communications 2021, **42**:763–771

Keywords: 18F-labeled fluoroazomycinarabinoside, biomarkers, carbonic anhydrase IX, glucose transporter-1, high-grade glioma, hypoxia, hypoxia-inducible factor, immunohistochemistry, PET/CT

[a]Vita-Salute San Raffaele University, [b]Nuclear Medicine Department, [c]Pathology Unit, [d]Neuroradiology Unit and CERMAC, [e]Department of Neurosurgery and Gamma Knife Radiosurgery, IRCCS San Raffaele Scientific Institute and [f]University Centre of Statistics in the Biomedical Sciences, Vita-Salute San Raffaele University, Milan, Italy

Correspondence to Maria Picchio, MD, Nuclear Medicine Department, IRCCS San Raffaele Scientific Institute, Via Olgettina 60, 20132 Milan, Italy
Tel: +39 02 2643 6117; fax: +39 02 2641 2717; e-mail: picchio.maria@hsr.it

Received 30 October 2020 **Accepted** 28 January 2021

Introduction

Hypoxia is a biological condition frequently associated with malignant tumours and high-grade glioma (HGG), the most frequent primary brain tumour, is a significantly hypoxic neoplasia [1].

A correlation between hypoxia and aggressive behaviour in HGG has been demonstrated, as well as its association with poor prognosis and resistance to both chemo- and radiotherapy [2–4].

In order to non-invasively define the tumour regions with a higher degree of hypoxia, the use of reliable imaging modalities is advocate, as this approach might improve the diagnostic work-up by guiding specific bioptic sampling and by supporting radiation treatment planning with the delivery of higher doses on the most hypoxic tumour regions [5–7].

MRI is currently performed to investigate angiogenesis and tumour vasculature, but it does not provide specific information regarding hypoxia.

PET/computed tomography (PET/CT), using specific radiotracers targeting distinct molecular pathways, has been increasingly used to investigate gliomas, and specifically HGG [8,9].

Next to radiotracers investigating tumour metabolism and proliferation such as ^{18}F-fluorodeoxyglucose

0143-3636 Copyright © 2021 Wolters Kluwer Health, Inc. All rights reserved. DOI: 10.1097/MNM.0000000000001396

(^{18}F-FDG), ^{18}F-fluoroethyl-L-tyrosine (^{18}F-FET), ^{18}F-fluorothymidine (^{18}F-FLT) and ^{11}C-Methionine (^{11}C-MET), hypoxia radiotracers have been also tested in this setting.

The most widely used hypoxia radiotracer, ^{18}F-fluoromisonidazole (^{18}F-FMISO), which is trapped in hypoxic cells due to a consequent reduction process allowing a covalent binding into intracellular macromolecules, showed uptake proportional to the level of hypoxia and its retention seemed to be correlated to the measurement performed using invasive polarographic oxygen electrodes [10,11].

Another radiotracer that has been proposed and tested for clinical purposes in different types of cancer is ^{18}F-labeled fluoroazomycinarabinoside (^{18}F-FAZA), which has several advantages over ^{18}F-FMISO in terms of kinetic properties [12–18].

From a molecular point of view, during hypoxic conditions, the α-subunit of hypoxia-inducible factor 1α (HIF-1α) is activated and binds to the subunit HIF-1β, leading to the composition of the heterodimeric HIF-1, which regulates the transcription of several genes, including vascular endothelial growth factor (VEGF), glycolytic enzymes, glucose transporter-1 (GLUT-1) and carbonic anhydrase IX (CA-IX) [11].

Significant but weak correlations have been demonstrated between ^{18}F-FMISO standardised uptake value (SUV) and VEGF expression in newly diagnosed gliomas, but no correlation between ^{18}F-FMISO SUV and HIF-1α expression nor between hypoxic volume and tissue/blood ratio has been demonstrated [4,11].

To the best of our knowledge, there are no available studies investigating the correlations between ^{18}F-FAZA PET/CT-derived parameters and hypoxia immunohistochemical biomarkers in HGG.

The present study aims to investigate the likelihood of correlations between ^{18}F-FAZA uptake and immunohistochemical biological markers of hypoxia in newly diagnosed patients with HGG.

Materials and methods

Patients

In this prospective clinical study, 20 patients with brain MRI suggestive for HGG have been enrolled from April 2016 to October 2017 at Istituto di Ricovero e Cura a Carattere Scientifico (IRCCS) San Raffaele Scientific Institute. All recruited patients underwent ^{18}F-FAZA PET/CT before starting treatment, with the exception of two patients dropped out because of technical issues regarding radiotracer synthesis. Among the 18 patients who underwent a baseline scan, 4/18 also underwent a further ^{18}F-FAZA PET/CT for suspected recurrence, according to the clinical protocol. Patients' recruitment started after the approval by the Institutional Ethics Committee of IRCCS San Raffaele Scientific Institute (EudraCT: 2015-000679-28); each patient signed an informed consent form to participate to the study.

PET/CT image acquisition

^{18}F-FAZA radiotracer has been produced according to a previously described procedure [19]. Each patient was administered with an intravenous injection of 372 ± 17 (range: 340–407) MBq of ^{18}F-FAZA. The PET/CT scan has been performed on a Discovery 690 (General Electric Medical Systems), and the acquisition started 120 min after tracer injection with 3D mode acquisition. PET images have been reconstructed using an iterative algorithm (ordered subset expectation maximization = OSEM; subsets = 18; iterations = 5; transaxial post-filter – Gaussian with full width half maximum = 2 mm; axial filter = standard; time of flight and point spread function model = ON; reconstructed field of view = 256 mm; image matrix = 256 × 256). Attenuation correction was performed using CT images, after the conversion of the CT numbers in linear attenuation coefficients for the 511 keV energy radiation. Correction for dead-time, random and scatter events have also been performed.

PET/CT image analysis

Image analysis has been carried out on an Advantage WorkStation (General Electric Medical Systems) and using PMOD software (PMOD Technologies Limited Liability Company).

Two nuclear medicine physicians reported the scan for each patient and every tracer accumulation deviating from the physiological distribution was regarded as positive for the presence of hypoxia.

Three volume of interest corresponding to 40, 50 and 60% of the maximum standardised uptake value (SUV_{max}) was defined. Beside the SUV_{max}, the other following parameters were measured: mean standardised uptake value (SUV_{mean}) and ^{18}F-FAZA tumour volume (FTV).

Different threshold of tumour-to-blood ratio (T/B) has been applied and tested, namely T/B>1.2, T/B>1.3 and T/B>1.4. For each of the resulting hypoxia regions, the corresponding hypoxic volume was measured as hypoxic volume1.2, 1.3 and 1.4.

Tissue samples and immunohistochemical analysis

All patients underwent surgery at the Neurosurgery Department of the IRCCS San Raffaele Scientific Institute.

A stereotactic biopsy was performed in 10 out of 18 patients. The procedure began with the fixation to the patient's skull of the MRI-compatible Leksell stereotactic frame (Model G, Elekta), with the aid of local anaesthetic and mild intravenous sedation. A contrast-enhanced axial

3D-T1 MRI (voxel 1×1 mm, slice thickness 1 mm without gap, matrix 256×256 mm) was then obtained, with the appropriate fiducial system, on a Philips Achieva 1.5T MR scanner (Philips Medical Systems, Best, the Netherlands). A 3D T2-weighted series was also acquired in most cases. Relevant imaging and parameter maps (including ^{18}F-FAZA PET/CT) were imported into the dedicated software for stereotactic planning Leksell SurgiPlan (Elekta Instruments AB, Stockholm, Sweden) and co-registered to the newly acquired stereotactic images. After careful planning, with the definition of biopsy target sites and path, the patient was placed in the operating room and positioned semi-sitting or supine, with the patient's head and stereotactic frame fixed to the operating table. Stereotactic coordinates (x, y and z) and trajectory (arc and ring) calculated with SurgiPlan software were then used to set the intraoperative stereotactic system and guide the bioptic sampling. After preparation, drape and under local anaesthesia, a skin incision and skull burr hole were made according to the trajectory. A Sedan biopsy needle (10 mm needle windows, 2.5 mm diameter) was then inserted and at least two cylindrical tissue specimens (range 2–4, median 3) based on the macroscopical aspect and size of the sample, were taken for biopsy (median length 8 mm, range 4–11 mm). Care was taken in obtaining at least one sample from the area of high ^{18}F-FAZA uptake.

The tissue samples were immediately fixed in a 10% formalin solution and sent to the pathology department, where they were processed the same day, or the day after in case samples were sent late in the afternoon. At the end of the procedure, the frame was removed, and a CT scan was performed. The bioptic sampling accuracy was confirmed via co-registering the postoperative CT images with preoperative imaging and planned trajectory in the SurgiPlan software for all cases in the series.

For the eight patients who underwent craniotomy and surgical tumour resection, two pathologists reviewed slides and selected the most representative histological tumour section for the subsequent analysis. Histopathological diagnosis was performed according to the 2016 WHO. For 2 out of 10 patients who underwent bioptic sampling, it was not possible to perform both molecular and cytogenetic studies and the diagnosis was made by morphological criteria only.

Routine haematoxylin and eosin staining and all available formalin-fixed paraffin-embedded (FFPE) tumour tissue blocks were retrieved. For each case, we evaluated three hypoxia markers (HIF-1α, CA-IX and GLUT-1), angiogenesis tumour status and proliferative tumour index.

Tissue samples and immunohistochemical analysis

Immunohistochemistry was carried out using Tris-EDTA pH 9.0 for antigen retrieval and a high sensitivity polymer-based HRP as a detection system, using the DAB chromogen. For HIF-1α, a rabbit mAb (clone EP1215Y) from Abcam diluted 1:1000 was used, CA-IX expression was evaluated using a rabbit mAb by Ventana Roche (clone EP161) diluted 1:800, and for GLUT-1, a pre-diluted rabbit polyclonal antibody from Ventana was used.

For both CA-IX and GLUT-1 assessment, antibodies produced by Ventana Roche (Cell Marque) were used, both sold as in-vitro diagnostic (IVD) reagent; for both antibodies, detection techniques were performed using IVD reagents. Also, for each single run, positive hypoxic control tissue (clear cell renal cell carcinoma) was used.

Tumour vascularity was studied using a pre-diluted anti-CD31 mouse mAb (clone JC70) from Cell Marque; for proliferative tumour index, a pre-diluted anti-Ki-67 (clone 30-9) rabbit mAb from Ventana was used.

Regardless of the sample, the evaluation of immunostainings was performed by applying the same scoring systems for both resections and biopsies. To strengthen the applied methodology and to better investigate hypoxia marker heterogeneity within a tumour, we broadened the scope of our study of surgical resection samples evaluating GLUT-1, CA-IX and HIF-1α on all tumour sections available for each case.

Immunostaining was performed on adjacent five micron-thick tumour sections; to evaluate the extent of CA-IX and GLUT-1 tumour cells expression, a semiquantitative scoring system was implemented, according to five categories (0 = 0%; 1 ≤ 10%; 2 = 11–25%; 3 = 26–50% and 4 = 51–75%) [20] and recorded respectively as 0, 1, 2, 3 and 4. HIF-1α nuclear immunoreactivity in neoplastic cells was reported as absent (0), focal (1) and plurifocal (2).

Tumour vascularity was quantified referring to the so-called hot-spots method [21]. For each tumour slide, three fields containing the highest vessel number were selected and then vessels were counted at high power (40×); finally, a vessel number average count was obtained. We did not differentiate normal from hyperplastic or proliferative vessels.

Immunomarker expression assessment was independently and manually performed by two pathologists blinded to PET analysis.

Statistical analysis

Correlations between all PET-derived parameters and anatomopathological features (CA-IX, GLUT-1, average number of capillaries, anti-CD31 antibody and Ki-67) were evaluated by using the nonparametric Spearman's correlation coefficient. For patients with multiple lesions, only PET data of the main lesion were used for computing the correlations. The correlation analysis was performed separately for the two subgroups (surgical and bioptic). The descriptive statistics of the time of follow-up were based on the analysis of the time to censoring.

P values lower than 0.05 were considered significant. Statistical analyses were performed using R 3.5.0 (http://www.R-project.org/).

Results

Patients

The study population consisted of 13 male and 5 female patients, with a mean age of 66 years (range 41–81).

Ten out of 18 patients underwent stereotactic biopsy, and 8/18 underwent craniotomy with surgical excision of the lesion. According to WHO classification, 12/18 patients had grade IV glioma and 5/18 had grade III glioma (three anaplastic astrocytomas and two anaplastic oligodendrogliomas); one patient was diagnosed with brain metastases from lung cancer, thus subsequent immunohistochemistry analyses were performed on the 17 patients presenting a final histological diagnosis of HGG. Patients' characteristics can be found in Table 1.

Table 1 Patients' characteristics

Patient	Age (years)	Sex	Histotype (WHO classification)	Sampling
01	77	Male	Glioma Grade IV	Biopsy
02	58	Male	Glioma Grade IV	Biopsy
03	57	Female	Glioma Grade IV	Biopsy
04	71	Female	Glioma Grade IV	Surgical resection
05	56	Male	Glioma Grade IV	Surgical resection
06	77	Male	Glioma Grade IV	Surgical resection
07	64	Male	Glioma Grade III	Biopsy
08	81	Male	Glioma Grade III	Biopsy
09	61	Male	Glioma Grade IV	Surgical resection
10	79	Male	Glioma Grade IV	Surgical resection
11	44	Female	Glioma Grade IV	Biopsy
12	69	Female	Glioma Grade III	Biopsy
13	61	Male	Glioma Grade III	Surgical resection
14	41	Male	Glioma Grade III	Biopsy
15	65	Male	Glioma Grade IV	Surgical resection
16	64	Male	Glioma Grade IV	Biopsy
17	73	Female	Glioma Grade IV	Biopsy

^{18}F-FAZA PET/CT scans identified a single lesion in 15/17 patients and multiple lesions in 2/17 patients affected by HGG. The patient with the final diagnosis of brain metastases from lung cancer presented a positive ^{18}F-FAZA PET/CT, corresponding to the lesion. ^{18}F-FAZA PET/CT parameters for each patient are reported in Table 2.

Hypoxia factors immunohistochemical staining results

All tumour samples, except one, showed immunoreactivity for GLUT-1 expression. Two of 17 samples were scored as 1, 6/17 as score 2, 6/17 as score 3 and 2/17 as score 4 (Table 3).

Regarding CA-IX expression, the score analysis was as follows: 0 in 3/17 cases, 1 in 8/17 patients, 2 in 2/17 cases, 3 in 3/17 and 4 in 1/17.

Immunostaining for HIF-1α showed the following results: 0 in 2 patients, 1 in 12 patients and 2 in 3 patients. The mean Ki-67 value was 18% (range: 3–40%).

Tumour cells showed GLUT-1 cell membrane staining pattern and for CA-IX a cytoplasmic immunoreactivity was also detected (Fig. 1). GLUT-1 and CA-IX were predominantly expressed in perinecrotic pseudopalisading areas, in accordance with previous studies and

Table 2 ^{18}F-FAZA PET-derived parameters for each patient

Patient	Site of FAZA uptake	SUV_{max}	SUV_{mean} 40%	SUV_{mean} 50%	SUV_{mean} 60%	FTV 40%	FTV 50%	FTV 60%	Hypoxic volume(cc) Threshold 1.2	Hypoxic volume(cc) Threshold 1.3	Hypoxic volume(cc) Threshold 1.4
1	Right thalamus-capsular	3.5	2.0	2.2	2.4	4.41	3.00	1.72	3.35	2.81	2.31
2	Right frontal-posterior	2.5	1.5	1.6	1.8	3.02	3.23	1.4	1.21	0.8	0.47
3	Right temporal-insular	2.6	1.5	1.7	1.8	7.69	5.26	2.67	2.27	1.36	0.53
4	Left temporal-parietal	1.9	1.1	1.2	1.3	16.9	11.27	6.19	3.24	1.86	0.86
5	Left frontal	3.5	2.0	2.1	2.4	18.8	12.22	6.2	16.69	16.48	15.82
6	Left temporal	3.2	2.1	2.3	2.4	42.43	31.93	20.89	31.82	27.63	21.11
7	Trunk of corpus callosum	5.7	3.5	3.8	4.1	29.82	23.26	16.32	34.35	32.97	31.71
8	Right mesial temporal-occipital	2.6	1.6	1.7	1.8	29.97	22.76	14.55		8.89[a] 4.05[a] 1.21[a]	
	Right parietal superior	1.5	0.8	1.0	1.1	0.55	0.29	0.15			
	Left temporal	2.8	1.5	1.7	2.0	1.00	0.51	0.21			
9	Right temporal-parietal-occipital	2.6	1.5	1.7	1.8	21.89	15.3	8.14	10.99	8.77	6.1
10	Right temporal-parietal	4.2	2.4	2.7	2.9	50.63	36.65	21.10	45.99	36.35	27.03
11	Left frontal-parietal occipital and right parietal	3.2	1.7	1.9	2.2	15.16	7.13	2.13	15.05	13.61	11.28
12	Left frontal anterior lateral	1.1	0.6	0.7	0.8	1.16	0.58	0.26		0.54[b] 0.48[b] 0.39[b]	
	Left medial frontal anterior	4.8	2.9	3.3	3.6	0.49	0.34	0.23			
	Left frontal posterior	1.2	0.7	0.8	0.9	1.14	0.72	0.41			
13	Right temporal	2.4	1.4	1.6	1.8	0.74	0.45	0.28	1.22	1.08	0.97
14	Negative	Na	Na	Na	Na	Na	Na	Na	Na	Na	Na
15	Right fronto-temporal	1.8	1	1.2	1.3	11.14	4.54	2.35	0.34	0.09	0 (no hypoxic volume)
16	Left temporal	4.4	2.7	3.1	3.4	1.6	1.10	0.75	1.71	1.52	1.34
17	Right Frontal	4.2	2.1	2.5	2.8	38.34	12.54	4.23	18.4	11.49	7.4

[a]Total of 3 lesions.[b]Total of 4 lesions.

immunostaining intensity was evenly high in all cases (Fig. 2) [22].

Furthermore, the extent of GLUT-1 was slightly higher compared to CA-IX. However, a correlation between marker immunostaining was observed. Among bioptic samples, the extent of GLUT-1 and CA-IX staining was lower in anaplastic astrocytomas and anaplastic oligodendrogliomas compared to glioblastomas, a result that is in line with previously published studies [23].

HIF-1α nuclear staining intensity was consistently weak through all tumour samples. Despite this, all stained nuclei were considered as immunoreactive. In all 17 cases, HIF-1α immunoreactivity in some intra- and peritumoural inflammatory cells was observed. Neoplastic cell nuclear staining was mainly focal with a heterogeneous distribution, and it was detected in perinecrotic sites as well as outside necrotic areas (Fig. 3). The extent of HIF-1α immunoreactivity did not correlate with GLUT-1 and CA-IX immunoreactivity. Similar results regarding hypoxia markers immunostaining were previously reported by considering tumour sections of surgical resection cases only, and not by including both bioptic and surgical samples, as performed in the present study [23].

Although HIF-1α antibody from Abcam is for research use only, immunohistochemical expression of this protein (clone EP1215Y from Abcam) has been previously investigated in other tumour cells, such as breast cancer [24] and vocal fold lesions [25]. Also, as regards to gliomas, recent studies examined HIF-1α immunoreactivity in tissue from patient with glioblastoma [25,26].

Table 3 **Immunohistochemistry analysis**

Patients	HIF-1α	CA-IX	Ki67 (%)	GLUT-1	Mean number of vessels/3HPF	CD31
01	1	3	5	4	11	1
02	1	1	20	2	32	2
03	1	1	5	3	19	1
04	1	1	10	2	16	1
05	2	3	25	3	12	1
06	2	2	15	3	21	2
07	1	1	20	2	7	1
08	1	1	15	2	15	1
09	1	2	40	4	44	3
10	1	3	20	3	42	3
11	1	0	25	3	25	2
12	1	1	3	1	13	1
13	2	1	30	2	39	2
14	0	0	10	0	13	1
15	0	0	15	1	27	2
16	1	1	35	2	13	1
17	1	4	7	3	11	1

CA-IX, carbonic anhydrase IX; GLUT-1, glucose transporter-1; HIF, hypoxia-inducible factor; HPF, high power field.

Correlation between ^{18}F-FAZA PET/CT parameters and immunohistochemistry

A positive correlation between CA-IX and all PET-derived parameters was observed in the surgical subgroup ($n=7$). Specifically, the correlation (corr) was very high with SUV_{max} (corr = 0.9728; $P=0.0002$) and high with $SUV_{mean}40$ (corr = 0.8994; $P=0.0058$), $SUV_{mean}50$ (corr = 0.8798; $P=0.0090$), $SUV_{mean}60$ (corr = 0.8505; $P=0.0153$), FTV40–50–60 (corr = 0.7709; $P=0.0424$, for all parameters) and hypoxic volume1.2–1.3–1.4 (corr = 0.8994; $P=0.0058$, for all parameters).

Fig. 1

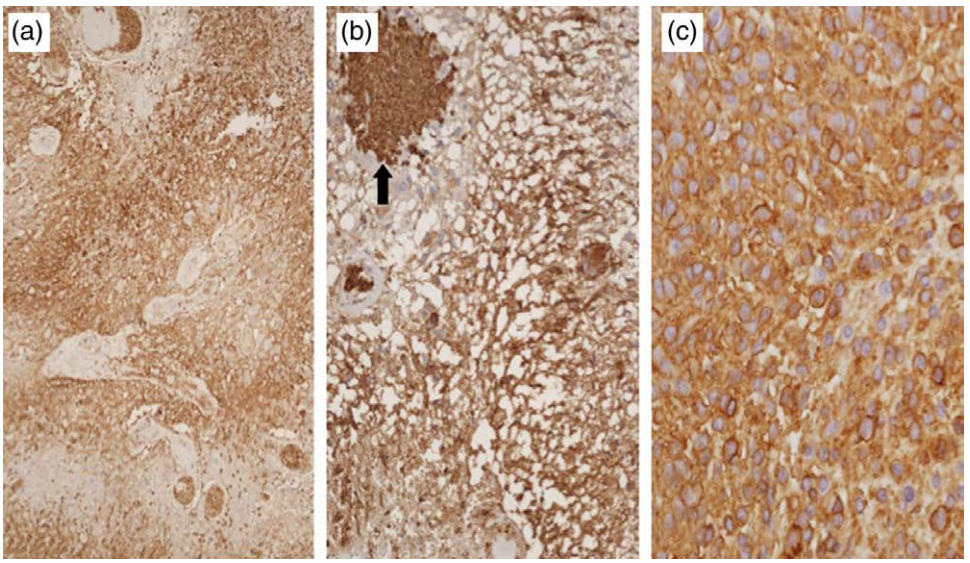

Glioblastoma formalin-fixed sample immunostained with anti-GLUT-1 antibody: images of strong and diffuse GLUT-1 immunoreactivity; staining is detected mostly in perinecrotic tumour areas (a, 20X); normal blood cells are also immunostained (b, 20X arrow); neoplastic cells immunoreactive with a predominant membranous staining pattern (c, 40X).

Fig. 2

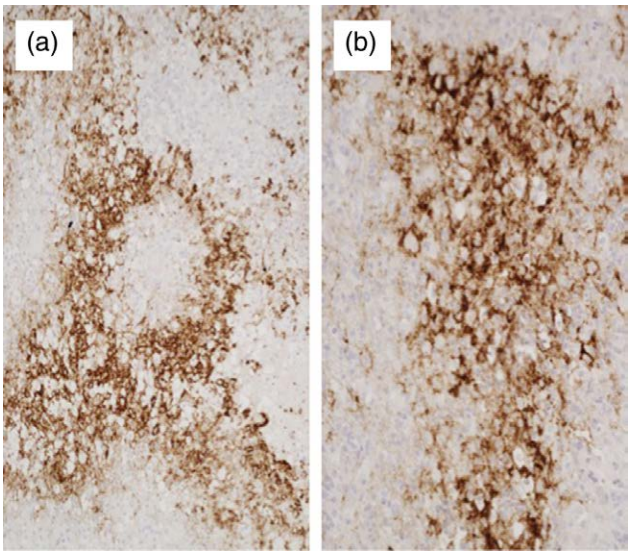

Glioblastoma formalin-fixed sample immunostained with anti-CA IX antibody. Images of strong and diffuse CA-IX immunoreactivity (a: 10X; b: 20X). Staining is detected in perinecrotic tumour areas with membranous and cytoplasmic granular staining pattern.

Fig. 3

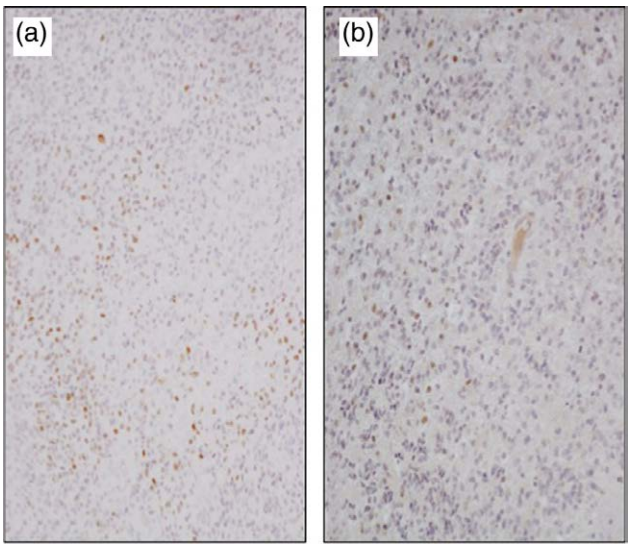

Glioblastoma formalin-fixed sample immunostained with anti-HIF1α antibody. Images of plurifocal (a, b, 20X) nuclear staining.

No correlations were observed between any PET-parameters and the extent of vascularisation.

Considering the bioptic subgroup ($n = 10$), a significant inverse correlation was observed between tumour vascularization and SUV_{max} (corr = –0.8017; $P = 0.0094$), $SUV_{mean}40$ (corr = –0.7933; $P = 0.0107$), $SUV_{mean}50$ (corr = –0.8017; $P = 0.0094$) and $SUV_{mean}60$ (corr = –0.7693; $P = 0.0154$) (Fig. 4 and Fig. 5).

Follow-up

The median follow-up was 192 days (interquartile range: 86.5–535). At the last follow-up, 11 patients were dead, 9/11 due to disease progression, 1/11 for pneumonia and herpetic encephalitis, whereas in 1/11, the cause of death was unknown because the patient completed the treatment in a different institution. Among the patients that were alive at last follow-up ($n = 5$), 4/5 showed stable disease, whereas for one patient, follow-up data were not available because of the patient's desire to be treated elsewhere.

Discussion

This is an exploratory study regarding 17 high-grade gliomas for which ^{18}F-FAZA PET/CT parameters were correlated to hypoxia marker immunohistochemical results and tumour vascularity.

The article herein describes a correlation between hypoxia imaging biomarkers derived from ^{18}F-FAZA PET/CT and immunohistochemical hypoxia markers. In particular, there were positive correlations between CA-IX and the degree of hypoxia defined by SUV_{max}, SUV_{mean} and hypoxic volume in the surgical subgroup.

These results are in accordance with previously published data using ^{18}F-FMISO as hypoxia radiotracer and with studies demonstrating positive correlations between hypoxia imaging and neoangiogenesis biomarkers. In fact, the abnormal structure and function of blood vessels that might occur during the angiogenetic process in glioblastoma ultimately leads to an ineffective perfusion, and thus to tumour hypoxia [23,27,28].

From our results, it seems that there is an inverse correlation between ^{18}F-FAZA uptake and CA-IX uptake in tumours collected by biopsies, whereas we found a strong correlation between ^{18}F-FAZA uptake and CA-IX in tumours from surgical resections. The evidence obtained from biopsies could be have been slightly affected by the study design, as we decided not to separate surgical samples from biopsies for the analysis. The most relevant issue that might have hampered the comparison analysis between samples and biopsies is represented by the amount of tissue representativity, which is related to the different way of sampling. Thus, to overcome this limit, we would like for the next future to extend our study to a larger cohort.

Similarly to the present paper, other studies demonstrated a direct correlation between angiogenesis markers, namely CD31 and CD34, and relative cerebral blood volume as determined by MRI studies [29].

Fig. 4

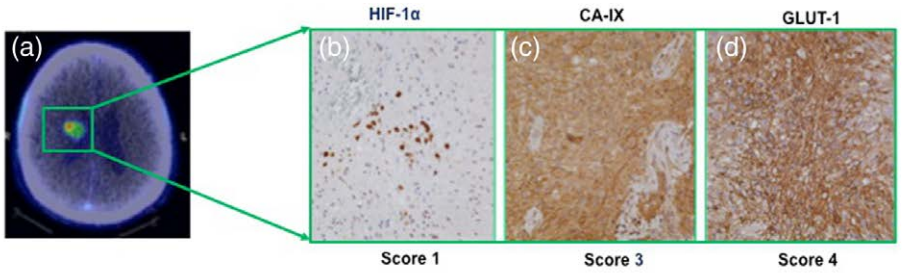

SUVmax	SUVmean 40%	SUVmean 50%	SUV mean 60%	FTV 40%	FTV 50%	FTV 60%	HV 1.2	HV 1.3	HV 1.4
3,5	2,0	2,2	2,4	4,41	3,00	1,72	3,35	2,81	2,31

77-year-old male patient (Patient no. 1) with GBM grade IV. ^{18}F-FAZA PET/CT (a) image shows radiotracer uptake in correspondence of the right thalamo-capsular lesion. Immunohistochemical analysis performed on the bioptic sample showed focal nuclear staining for HIF-1α (b), a diffuse immunoreactivity for CA-IX with a predominant membranous staining (c) and a diffuse and strong membranous staining pattern for GLUT-1 (d). Correspondent ^{18}F-FAZA PET-derived parameters are also reported in the bottom table.

Fig. 5

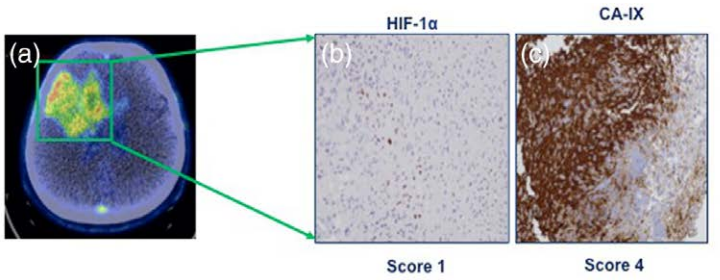

SUVmax	SUVmean 40%	SUVmean 50%	SUV mean 60%	FTV 40%	FTV 50%	FTV 60%	HV 1.2	HV 1.3	HV 1.4
4,2	2,1	2,5	2,8	38,34	12,54	4,23	18,40	11,49	7,40

73-year-old female patient (Patient no.17) with GBM grade IV. ^{18}F-FAZA PET/CT (a) image shows radiotracer uptake in correspondence of the right frontal lesion. Immunohistochemical analysis performed on the bioptic sample showed focal nuclear staining for HIF-1 α (b), a diffuse and strong membranous staining pattern for CA-IX (c). Correspondent ^{18}F-FAZA PET-derived parameters are also reported in the bottom table.

As CD31 is both a marker of normal and abnormal vessels, the inverse correlation described in the results between SUV_{max} and SUV_{mean} at different thresholds and vessel density in the bioptic sample might be due to the presence of a higher proportion of normal vessels rather than abnormal ones. However, it is expected that within a single tumour, there might be variations in the extent and degree of hypoxia, with concurrent variety of angiogenic patterns. This is particularly true for HGG, where bioptic sampling has clear limitations in describing intratumoural hypoxia heterogeneity, thus increasing the difficulty in correlating imaging, molecular and biological data.

Recently another HIFs α-subunit, HIF-2α, was investigated in gliomas. Unlike HIF-1α, which is mainly involved in acute hypoxia response, HIF-2α plays a significant role in chronic hypoxia conditions and tumour cells that can switch and activate in specific settings. It would be of interest to extend our study to HIF-2α expression in HGG, comparing it to HIF-1α immunohistochemical results.

Moreover, quantification measurement performed with immunohistochemistry is very challenging compared to more sensitive molecular biology approaches, thus representing an additional complication when correlations between imaging and biological data are performed [30].

Integrating histopathological tumour features and hypoxia immunomarker expression with molecular imaging analysis gives rise to the opportunity to better understand and characterise HGG. However, there are some limitations in this exploratory investigation; first, we assessed an immunohistochemical analysis both on surgical resection and stereotactic biopsies. This implies that for surgical resections, the pathologist was able to select the most representative tumour slide for hypoxia factors analysis; in contrast for biopsies, tissue availability was quantitatively much less. Second, the same immunoscore system was applied for surgical resection and biopsies, regardless of the amount of available tumour; nonetheless, we adopted a scoring system that could possibly be suitable for both surgical and biopsy specimens for all investigated markers.

Despite these limitations, based on the results of the present study and considering the very well-known heterogeneity characterising HGG at metabolic, molecular and genetic level, a noninvasive method able to provide a whole characterisation of hypoxia intratumor heterogeneity, such as ^{18}F-FAZA PET/CT, might be strategically essential for diagnostic and therapeutic targeting [31,32]. This is particularly true for radiotherapy treatment, as some studies have already started to suggest the potential relevance of hypoxia imaging in guiding bioptic sampling and radiotherapy treatment [5,6,33].

Conclusion

The correlation between imaging parameters deriving from ^{18}F-FAZA PET/CT and the immunohistochemical biomarkers CA-IX and CD31 represents a reliable method for assessing tumour hypoxia in HGG. The inverse correlation between tumour vascularisation and SUV_{max} and SUV_{mean} observed in patients undergoing bioptic sampling supports the hypothesis that highly vascularised tumours might present higher oxygen supply and therefore less hypoxia. The inclusion of both bioptic samples and surgical specimens in our cohort might have slightly hampered the analysis because of the different tissue representativity. Therefore, to overcome this limit, in the next future we will extend our study to larger cohorts of patients.

Acknowledgements

The present work was supported by the Italian Association for Cancer Research (grant IG 2014 Id.1524).
All procedures performed in studies involving human participants were in accordance with the ethical standards of the Institutional and national research committee and with the 1964 Helsinki Declaration and its later amendments or comparable ethical standards. In particular, patients' recruitment started after the approval by the Institutional Ethic Committee of San Raffaele Scientific Institute (EudraCT: 2015-000679-28).

Conflicts of interest

There are no conflicts of interest.

References

1 Rampling R, Cruickshank G, Lewis AD, Fitzsimmons SA, Workman P. Direct measurement of pO2 distribution and bioreductive enzymes in human malignant brain tumors. *Int J Radiat Oncol Biol Phys* 1994; **29**:427–431.
2 Evans SM, Judy KD, Dunphy I, Jenkins WT, Hwang WT, Nelson PT, *et al*. Hypoxia is important in the biology and aggression of human glial brain tumors. *Clin Cancer Res* 2004; **10**:8177–8184.
3 Flynn JR, Wang L, Gillespie DL, Stoddard GJ, Reid JK, Owens J, *et al*. Hypoxia-regulated protein expression, patient characteristics, and preoperative imaging as predictors of survival in adults with glioblastoma multiforme. *Cancer* 2008; **113**:1032–1042.
4 Spence AM, Muzi M, Swanson KR, O'Sullivan F, Rockhill JK, Rajendran JG, *et al*. Regional hypoxia in glioblastoma multiforme quantified with [18F] fluoromisonidazole positron emission tomography before radiotherapy: correlation with time to progression and survival. *Clin Cancer Res* 2008; **14**:2623–2630.
5 Mapelli P, Zerbetto F, Incerti E, Conte GM, Bettinardi V, Fallanca F, *et al*. 18F-FAZA PET/CT hypoxia imaging of high-grade glioma before and after radiotherapy. *Clin Nucl Med* 2017; **42**:e525–e526.
6 Mapelli P, Incerti E, Bettinardi V, Conte GM, Fallanca F, Bailo M, *et al*. Hypoxia 18F-FAZA PET/CT imaging in lung cancer and high-grade glioma: open issues in clinical application. *Clin Transl Imaging* 2017; **5**:389–397.
7 Vordermark D, Horsman MR. Hypoxia as a biomarker and for personalized radiation oncology. *Recent Results Cancer Res* 2016; **198**:123–142.
8 Derlon JM, Chapon F, Noël MH, Khouri S, Benali K, Petit-Taboué MC, *et al*. Non-invasive grading of oligodendrogliomas: correlation between *in vivo* metabolic pattern and histopathology. *Eur J Nucl Med* 2000; **27**:778–787.
9 Collet S, Valable S, Constans JM, Lechapt-Zalcman E, Roussel S, Delcroix N, *et al*. [(18)F]-fluoro-L-thymidine PET and advanced MRI for preoperative grading of gliomas. *Neuroimage Clin* 2015; **8**:448–454.
10 Lee ST, Scott AM. Hypoxia positron emission tomography imaging with 18f-fluoromisonidazole. *Semin Nucl Med* 2007; **37**:451–461.
11 Rasey JS, Koh WJ, Evans ML, Peterson LM, Lewellen TK, Graham MM, Krohn KA. Quantifying regional hypoxia in human tumors with positron emission tomography of [18F]fluoromisonidazole: a pretherapy study of 37 patients. *Int J Radiat Oncol Biol Phys* 1996; **36**:417–428.
12 Derlon JM, Cabal P, Blaizot X, Borha A, Chapon F. [Metabolic imaging for supratentorial oligodendrogliomas]. *Neurochirurgie* 2005; **51**:309–322.
13 Sorger D, Patt M, Kumar P, Wiebe LI, Barthel H, Seese A, *et al*. [18F] Fluoroazomycinarabinofuranoside (18FAZA) and [18F]Fluoromisonidazole (18FMISO): a comparative study of their selective uptake in hypoxic cells and PET imaging in experimental rat tumors. *Nucl Med Biol* 2003; **30**:317–326.
14 Picchio M, Beck R, Haubner R, Seidl S, Machulla HJ, Johnson TD, *et al*. Intratumoral spatial distribution of hypoxia and angiogenesis assessed by 18F-FAZA and 125I-Gluco-RGD autoradiography. *J Nucl Med* 2008; **49**:597–605.
15 Souvatzoglou M, Grosu AL, Röper B, Krause BJ, Beck R, Reischl G, *et al*. Tumour hypoxia imaging with [18F]FAZA PET in head and neck cancer patients: a pilot study. *Eur J Nucl Med Mol Imaging* 2007; **34**:1566–1575.
16 Piert M, Machulla HJ, Picchio M, Reischl G, Ziegler S, Kumar P, *et al*. Hypoxia-specific tumor imaging with 18F-fluoroazomycin arabinoside. *J Nucl Med* 2005; **46**:106–113.
17 Mapelli P, Incerti E, Fallanca F, Bettinardi V, Compierchio A, Masiello V, *et al*. Concomitant lung cancer and gastrointestinal stromal tumor: first report of hypoxia imaging with 18F-FAZA PET/CT. *Clin Nucl Med* 2017; **42**:e349–e351.
18 Mapelli P, Bettinardi V, Fallanca F, Incerti E, Compierchio A, Rossetti F, *et al*. 18F-FAZA PET/CT in the preoperative evaluation of NSCLC: comparison with 18F-FDG and immunohistochemistry. *Curr Radiopharm* 2018; **11**:50–57.
19 Savi A, Incerti E, Fallanca F, Bettinardi V, Rossetti F, Monterisi C, *et al*. First evaluation of PET-based human biodistribution and dosimetry of 18F-FAZA, a tracer for imaging tumor hypoxia. *J Nucl Med* 2017; **58**:1224–1229.

20 Hu M, Xing L, Mu D, Yang W, Yang G, Kong L, Yu J. Hypoxia imaging with 18F-fluoroerythronitroimidazole integrated PET/CT and immunohistochemical studies in non-small cell lung cancer. *Clin Nucl Med* 2013; **38**:591–596.
21 Fox SB, Harris AL. Histological quantitation of tumour angiogenesis. *APMIS* 2004; **112**:413–430.
22 Komaki S, Sugita Y, Furuta T, Yamada K, Moritsubo M, Abe H, *et al*. Expression of GLUT1 in pseudopalisaded and perivascular tumor cells is an independent prognostic factor for patients with glioblastomas. *J Neuropathol Exp Neurol* 2019; **78**:389–397.
23 Mayer A, Schneider F, Vaupel P, Sommer C, Schmidberger H. Differential expression of HIF-1 in glioblastoma multiforme and anaplastic astrocytoma. *Int J Oncol* 2012; **41**:1260–1270.
24 Cerci SM, Bozkurt KK, Eroglu HE, Cerci C, Erdemoglu E, Bulbul PT, *et al*. Evaluation of the association between HIF-1α and HER-2 expression, hormone receptor status, Ki-67 expression, histology and tumor FDG uptake in breast cancer. *Oncol Lett* 2016; **12**:3889–3895.
25 Rzepakowska A, Żurek M, Grzybowski J, Pihowicz P, Górnicka B, Niemczyk K, Osuch-Wójcikiewicz E. Microvascular density and hypoxia-inducible factor in intraepithelial vocal fold lesions. *Eur Arch Otorhinolaryngol* 2019; **276**:1117–1125.
26 Potharaju M, Mathavan A, Mangaleswaran B, Patil S, John R, Ghosh S, *et al*. Clinicopathological analysis of HIF-1alpha and TERT on survival outcome in glioblastoma patients: a prospective, single institution study. *J Cancer* 2019; **10**:2397–2406.
27 Liao D, Johnson RS. Hypoxia: a key regulator of angiogenesis in cancer. *Cancer Metastasis Rev* 2007; **26**:281–290.
28 Bekaert L, Valable S, Lechapt-Zalcman E, Ponte K, Collet S, Constans JM, *et al*. [18F]-FMISO PET study of hypoxia in gliomas before surgery: correlation with molecular markers of hypoxia and angiogenesis. *Eur J Nucl Med Mol Imaging* 2017; **44**:1383–1392.
29 Majchrzak K, Kaspera W, Szymaś J, Bobek-Billewicz B, Hebda A, Majchrzak H. Markers of angiogenesis (CD31, CD34, rCBV) and their prognostic value in low-grade gliomas. *Neurol Neurochir Pol* 2013; **47**:325–331.
30 Vartanian A, Singh SK, Agnihotri S, Jalali S, Burrell K, Aldape KD, Zadeh G. GBM's multifaceted landscape: highlighting regional and microenvironmental heterogeneity. *Neuro Oncol* 2014; **16**:1167–1175.
31 Quartuccio N, Laudicella R, Mapelli P, Guglielmo P, Pizzuto DA, Boero M, *et al*. Hypoxia PET imaging beyond 18F-FMISO in patients with high-grade glioma: 18F-FAZA and other hypoxia radiotracers. *Clin Transl Imaging* 2020; **8**:11–20.
32 Mapelli P, Picchio M. 18F-FAZA PET imaging in tumor hypoxia: a focus on high-grade glioma. *Int J Biol Markers* 2020; **35**:42–46.
33 Mapelli P, Fallanca F, Scifo P, Barbera M, Castellano A, Bettinardi V, *et al*. Hypoxia and amino acid imaging of high-grade glioma: 18F-FAZA PET/CT and 11C-Methionine PET/MRI. *Clin Nucl Med* 2020; **45**:e290–e293.